Journal of Applied Mechanics and Technical Physics, Vol. 44, No. 2, pp. 212–220, 2003

STABILITY AND TRANSITION ON A SWEPT CYLINDER IN A SUPERSONIC FLOW

A. I. Semisynov,[1] A. V. Fedorov,[2] V. E. Novikov,[1] N. V. Semionov,[1] and A. D. Kosinov[1]

UDC 532.526

Results of experimental investigations of the evolution of natural disturbances and laminar–turbulent transition in a supersonic boundary layer on the attachment line of a circular cylinder with a sweep angle of 68° *and a free-stream Mach number* M = 2 *are presented. The experimental studies are supplemented by calculations of the mean flow and stability characteristics. Flow regimes in the boundary layer on the attachment line are determined by a hot-wire technique as functions of the Reynolds number and height of two-dimensional roughness elements. The results are compared with* NASA (Ames) *experiments.*

Key words: *boundary layer, transition, stability, attachment line on a swept wing.*

It is known that the laminar–turbulent transition in a boundary layer on a swept wing is largely determined by the surface quality and boundary-layer flow character in the vicinity of the leading edge. The data obtained in studying the possibility of controlling the laminar flow [1–5] show that it is next to impossible to laminarize the flow on a swept wing if the boundary layer on the attachment line becomes turbulent. The wave processes that occur on the leading-edge attachment line and are responsible for transition to turbulence have not yet been adequately studied, which complicates solving the problem of boundary-layer laminarization on swept wings.

The transition on the attachment line has been mainly studied experimentally. In these studies, the critical values of the transition Reynolds number were determined. The experiments on swept cylinders for low flow velocities are reviewed in [6]. The investigations [6–8] of the boundary-layer transition on the attachment line with trip wires of different diameters revealed the complex behavior of disturbances. The following specific features were identified.

In the case of a "pure" flow (low levels of external disturbances and small roughness of the wetted surface), the initial phase of the transition process is characterized by amplification of unstable wave packets and can be studied using the linear theory of stability. A simplified analysis [7] based on the linear theory for a parallel incompressible flow predicts the critical Reynolds number based on the momentum thickness $\mathrm{Re}_{\theta,\mathrm{cr}} \approx 270$. Hall et al. [9] examined the stability of the swept Hiemenz flow and considered a particular family of two-dimensional solutions [called the HMP (Holl–Malik–Poll) mode below] related to plane waves propagating along the attachment line. The calculations showed that the critical Reynolds number was $\mathrm{Re}_{\theta,\mathrm{cr}} \approx 235$, which is in good agreement with the experiments of [7, 10]. Lin and Malik [11] developed an approach for determining three-dimensional boundary-layer stability on the attachment line on the basis of linearized stability equations for an incompressible flow. The use of this method in analyzing the Hiemenz flow stability revealed families of unstable three-dimensional modes (symmetric and antisymmetric) in addition to the HMP mode. Numerical results showed that the HMP mode is the first symmetric mode with the highest growth rate. Kazakov [12, 13] considered the HMP mode stability for a compressible swept Hiemenz flow. The possibility of controlling this type of instability with the help of heat addition to the boundary layer was considered in [14].

[1]Institute of Theoretical and Applied Mechanics, Siberian Division, Russian Academy of Sciences, Novosibirsk 630090. [2]Moscow Physicotechnical Institute, Zhukovskii, Moscow Region 140160. Translated from Prikladnaya Mekhanika i Tekhnicheskaya Fizika, Vol. 44, No. 2, pp. 72–82, March–April, 2003. Original article submitted May 27, 2002; revision submitted October 14, 2002.

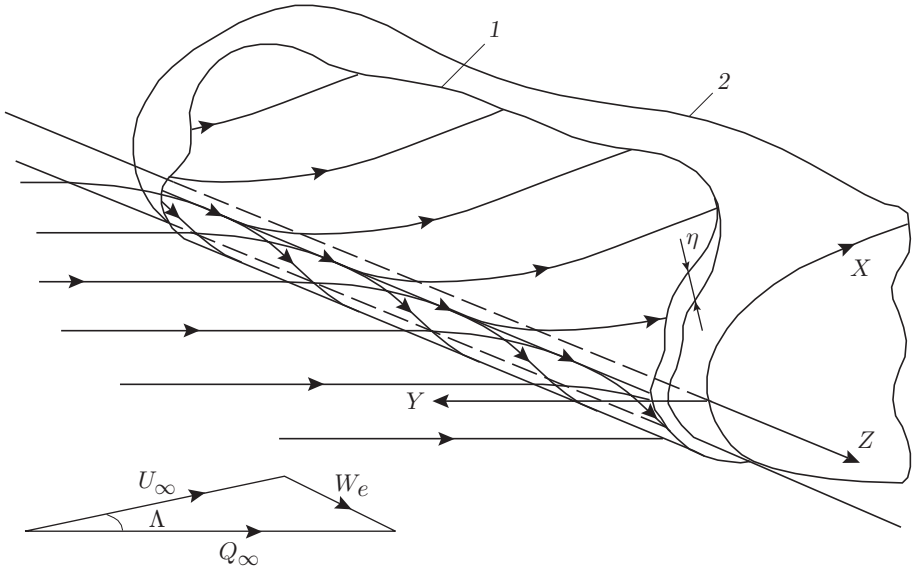

Fig. 1. Attachment line on a swept wing: surface streamlines (1) and swept wing surface (2).

Apparently, the boundary layer transition under intense external disturbances or in the case of a rough surface occurs via the nonlinear stage only. Theoretical investigations of this regime include the nonlinear stability analysis [15] and direct numerical simulation [16, 17].

Figure 1 shows schematically the flow around a swept wing (cylinder), coordinate system, and velocity components. The leading edge of the wing is called subsonic if the Mach number normal to the edge is $M_n < 1$ and supersonic if $M_n > 1$. To find the specific features of the laminar–turbulent transition on the leading edge of the swept wing, we considered the evolution of natural disturbances on the attachment line of a circular cylinder with a sweep angle of 68° with a Mach number M = 2, which corresponds to a subsonic leading edge. In addition, the mean flow in the boundary layer and the characteristics of its stability were calculated.

Statement of Experiments. The experiments were performed in a T-325 low-turbulent supersonic wind tunnel of the Institute of Theoretical and Applied Mechanics of the Siberian Division of the Russian Academy of Sciences. The main characteristics of the wind tunnel are described in [18, 19].

The models were circular cylinders made of steel, 38.4 mm in diameter and 145 or 530 mm long. One of the cylinders was mounted in the wind-tunnel test section at an angle of 68° to the incoming stream. The short cylinder was fixed on a traversing gear providing upstream and downstream displacements within 0.1 mm, and the long cylinder was rigidly attached to the side wall of the test section of the T-325 wind tunnel. The roughness was obtained using wires 0.075 and 0.115 mm in diameter for the first model and 0.2, 0.3, 0.44, 0.54, 0.83, and 1.12 mm for the second model. The wire was glued over the cylinder circumference at a distance of 45 and 220 mm from the apex for the short and long cylinders, respectively.

An automated data acquisition system similar to that described in [20] was used in the experiments. The mean and fluctuating characteristics of the flow were measured by a constant-temperature anemometer with a 1 : 10 ratio of arms and a frequency range up to 400 kHz [20] and by tungsten-wire probes 5 μm in diameter and 1 mm long. The wire overheating was 0.8, and the measured disturbances corresponded to mass-flow fluctuations [20, 21]. The fluctuating voltage from the hot-wire anemometer was fed to a computer by a 12-digit analog-to-digital converter (ADC) with a frequency of 750 kHz. Digital oscillograms contained 16,384 points. The mean voltage from the hot-wire anemometer was recorded into the computer through input registers connected to a ShCh1516 voltmeter. The probe was fixed on the traversing gear and moved at an angle of 68° to the Y axis with accuracy of 0.01 mm. The initial value of this coordinate (probe position relative to the model) was determined by electric contact of the probe and the cylinder surface.

Theoretical Analysis. Since the characteristic Reynolds number based on the boundary-layer thickness and flow parameters at the boundary-layer edge is rather high, the asymptotic method of multiple scales can be used to analyze flow stability at the attachment line [22, 23]. This method is based on the fact that the boundary-layer

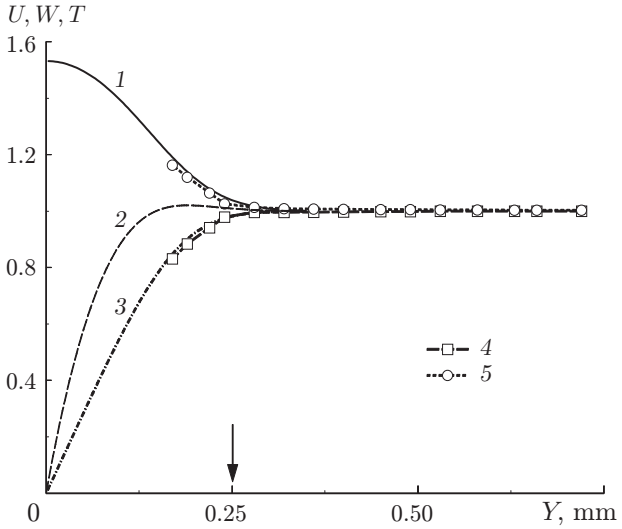

Fig. 2. Mean-flow profiles on the attachment line: curves 1–3 show the calculated data for T (1), U (2), and W (3); points 4 and 5 refer to the experimental data for W (4) and T (5).

thickness δ is much smaller than the characteristic longitudinal scale L. In the case of the flow on the attachment line, L is the leading-edge radius, and the small parameter can be defined as $\varepsilon = 1/\,\mathrm{Re}$, where $\mathrm{Re} = \eta^* W_e^*/\nu_e^*$ is the Reynolds number and $\eta^* = \sqrt{\nu_e^*/(\partial U_e^*/\partial X)|_{X=0}}$ is the scale of the boundary-layer thickness. The flow on the attachment line in the Z direction is parallel (Fig. 1). Still, it is not parallel in the chord direction X because of the boundary-layer growth and curved surfaces and streamlines. The effect of nonparallelism is considered as a small (of the order of $1/\,\mathrm{Re}$) perturbation of the mean flow.

Mean Flow. Boundary-layer characteristics are assumed to be constant in the Z direction. For low values of η^*/L, the cylinder-surface curvature can be neglected. Then, the coordinate system (X, Y, Z) in the vicinity of the attachment line is locally Cartesian. The velocity components, temperature, and pressure are presented as

$$(u, v, w)(x, y, z) = (\varepsilon x U(y), \varepsilon V(y), W(y)), \quad T = T_0(y), \quad P = (\gamma \mathrm{M}_e^2)^{-1} - \varepsilon^2 x^2/2,$$

where the quantity η^* is used to normalize the coordinates x, y, z, the velocity is normalized to W_e^*, and the temperature and pressure are normalized to T_e^* and $\rho_e^* W_e^{*2}$, respectively; $\gamma = 1.4$ is the ratio of specific heats and $\mathrm{M}_e = W_e/a_e$ is the local Mach number. For a thermoinsulated surface, the profiles $U(y)$, $V(y)$, $W(y)$, and $T(y)$ are solutions of the following system of ordinary differential equations [1, 2]:

$$(U^2 + VU')/T_0 = 1 + \mu' T' U' + \mu U'', \qquad VW'/T = \mu' T' W' + \mu W'',$$

$$U - VT'/T + V' = 0, \qquad \mu' T'^2/\mathrm{Pr} + \mu T''/\mathrm{Pr} - T' V/T + \mathrm{M}_e^2(\gamma - 1)\mu W'^2 = 0,$$

$$U(0) = W(0) = V(0) = 0, \quad T'(0) = 0, \quad y = 0, \qquad U(\infty) = W(\infty) = T(\infty) = 1.$$

Here $\mathrm{Pr} = 0.72$ is the Prandtl number and $\mu = \mu^*/\mu_e^*$ is the dimensionless viscosity calculated by the Sutherland formula.

Flow characteristics at the boundary-layer edge were calculated by the Euler equations for the following test conditions: a cylinder 38.4 mm in diameter with a sweep angle $\Lambda = 68^\circ$ is exposed to the flow, the free-stream Mach number is $\mathrm{M}_\infty = 2$, and the stagnation temperature is $T_0 = 310$ K. Calculations with ignored viscosity yields the local Mach number $\mathrm{M}_e = 1.76$ and temperature $T_e = 191.6$ K.

The boundary-layer equations were integrated with a unit Reynolds number $\mathrm{Re}_{\infty,1} = 6.75 \cdot 10^6$ m^{-1}, which corresponds to a Reynolds number $\mathrm{Re} = 537$ and boundary-layer thickness scale $\eta^* = 7.23 \cdot 10^{-5}$ m. The theoretical profiles of the mean flow are shown in Fig. 2. The arrow indicates the boundary-layer thickness $\delta \approx 0.25$ mm determined from the experimental mean-velocity profile plotted in Fig. 2. This value is in agreement with the calculated one.

Stability Characteristics. The instantaneous flow field is represented as $Q(x, y, z, t) = Q_0(x, y) + q(x, y, z, t)$, where the quantity $Q_0 = (\varepsilon x U, \varepsilon V, W, P, T)$ characterizes the mean flow and $q = (u, v, w, p, \theta)$ are velocity, pressure,

and temperature disturbances. Defining the slow variables by the relations $x_1 = \varepsilon x$, $z_1 = \varepsilon z$, and $t_1 = \varepsilon t$, we consider oblique waves with given wavenumbers α and β on the attachment line $x_1 = 0$. In this case, the disturbance vector we write as

$$F = \Big(u, \frac{\partial u}{\partial y}, v, p, \theta, \frac{\partial \theta}{\partial y}, w, \frac{\partial w}{\partial y}\Big)^{\mathrm{t}},$$
$$F(x, y, z, t) = [Z_0(t_1, y) + \varepsilon Z_1(t_1, y) + \ldots] \exp(i\alpha x + i\beta z - i\omega t), \tag{1}$$

where α and β are real wavenumbers and $\omega = \omega(\alpha, \beta)$ is a complex eigenvalue. The temporal growth is determined by the increment $\omega_i = \operatorname{Im}\omega$. Substituting (1) into the linearized Navier–Stokes equations, we obtain the following boundary-value problem in the main approximation in terms of ε:

$$\frac{\partial Z_0}{\partial y} = HZ_0,$$
$$Z_{01} = Z_{03} = Z_{05} = Z_{07} = 0, \quad y = 0, \qquad Z_{01}, Z_{03}, Z_{05}, Z_{07} \to 0, \quad y \to \infty. \tag{2}$$

The matrix H depends on the mean-flow profiles of x_1U, W, and T, Reynolds number Re, and wave characteristics α, β, and ω; it explicit form for a three-dimensional compressible boundary layer can be found in [22, 23]. The solution of problem (2) is represented in the form $Z_0 = C(t_1)\zeta(x_1, y; \alpha, \beta, \omega)$, where ζ is the eigen vector-function. In the next approximation in ε, we obtain the inhomogeneous problem

$$\frac{\partial Z_1}{\partial y} = HZ_1 + G_t \frac{\partial Z_0}{\partial t_1} + G_x \frac{\partial Z_0}{\partial x_1} + GZ_0,$$
$$Z_{11} = Z_{13} = Z_{15} = Z_{17} = 0, \quad y = 0, \qquad Z_{11}, Z_{13}, Z_{15}, Z_{17} \to 0, \quad y \to \infty, \tag{3}$$

where $G_x = -i\partial H/\partial\alpha$ and $G_t = i\partial H/\partial\omega$. The matrix G depending on the profiles of U and V and the flow variable x_1 describes the effect of mean-flow nonparallelism in the X direction. Problem (3) has nontrivial solutions if its right side is orthogonal to the eigenvector ξ of the problem conjugate to (2). This condition yields the equation for the amplitude coefficient

$$\frac{dC}{dt_1} = h_\omega C, \quad h_\omega = -\frac{1}{\langle G_t\zeta, \xi\rangle}\Big(\Big\langle G_x \frac{\partial \zeta}{\partial x_1}, \xi\Big\rangle + \langle G\zeta, \xi\rangle\Big), \quad \langle f, g\rangle \equiv \int_0^\infty (f, g)\, dy, \tag{4}$$

which has a solution $C = C_0 \exp(\varepsilon h_\omega t)$. The exponent εh_ω can be treated as a correction to the eigenvalue of $\omega(\alpha, \beta)$. Then, the complex frequency of the disturbance is determined as $\Omega = \omega + i\varepsilon h_\omega$.

Numerical calculations for two-dimensional waves ($\alpha = 0$) with low Mach numbers showed that the eigenvalues and eigenfunctions calculated by the asymptotic method with allowance for flow nonparallelism almost coincide with the corresponding results of [11]. In addition, the analysis of [9] was extended to the case of compressible flows. The exact solution for the HMP mode was compared to the asymptotic solution for supersonic flow velocities. Figure 3 shows an example of such a comparison for a Mach number $\mathrm{M}_e = 1.55$ and Reynolds number $\mathrm{Re} = 1000$. As in the case of low velocity of the flow, the asymptotic solution is in good agreement with the exact HMP solution.

Parametric calculations for three-dimensional disturbances showed that two-dimensional waves with $\alpha = 0$ are most unstable at low Mach numbers. For supersonic regimes $\mathrm{M}_e > 1$, the maximum increments correspond to three-dimensional traveling waves. The calculation results for a local Mach number $\mathrm{M}_e = 1.76$ and temperature $T_e = 191.6$ K corresponding to test conditions are plotted in Fig. 4. For $\mathrm{Re} < 520$, the boundary layer on the leading edge is stable. For $\mathrm{Re} > 520$, the phase velocity of the most unstable waves is $c = \omega_r/\beta \approx 0.5$; the angles of inclination of the wave vector $\psi = \arctan(\alpha/\beta)$ vary from 43° for $\mathrm{Re} = 520$ to 51° for $\mathrm{Re} = 1000$.

In a similar manner, we consider monochromatic waves with a fixed frequency ω and wavenumber α. The solution of problem (2) is represented as $Z_0 = C(z_1)\zeta(x_1, y; \alpha, \beta, \omega)$, where $\beta = \beta(\alpha, \omega)$ is a complex eigenvalue. Equation (4) acquires the form

$$\frac{\partial Z_1}{\partial y} = HZ_1 + G_z \frac{\partial Z_0}{\partial z_1} + G_x \frac{\partial Z_0}{\partial x_1} + GZ_0,$$

where $G_z = -i\partial H/\partial\beta$. The amplitude function is the solution of the equation

$$\frac{dC}{dz_1} = h_\beta C, \qquad h_\beta = -\frac{1}{\langle G_z\zeta, \xi\rangle}\Big(\Big\langle G_x \frac{\partial \zeta}{\partial x_1}, \xi\Big\rangle + \langle G\zeta, \xi\rangle\Big).$$

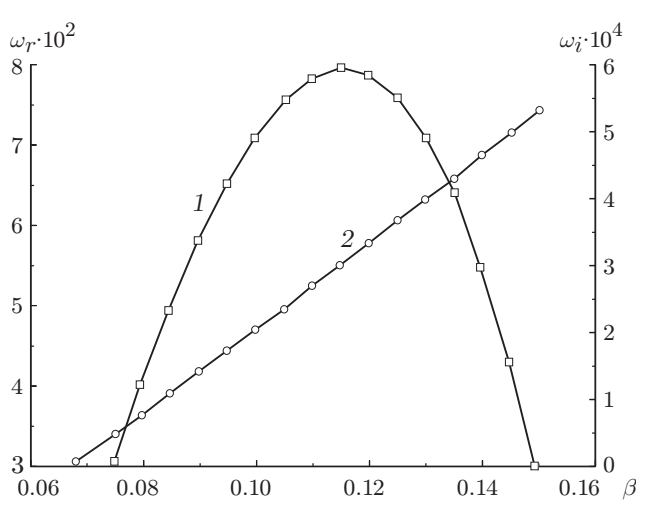

Fig. 3

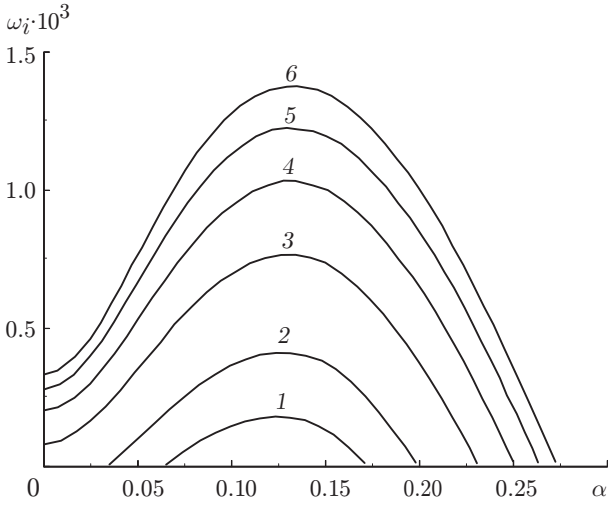

Fig. 4

Fig. 3. Eigenvalues of the HMP mode for $M_e = 1.55$, $Re = 1000$, and $\alpha = 0$: curves 1 and 2 refer to ω_i and ω_r, respectively; the curves show the exact solution and the points show the asymptotic solution.

Fig. 4. Maximum temporal increments ω_i for $Re = 550$ (1), 600 (2), 700 (3), 800 (4), 900 (5), and 1000 (6).

The growth rate of the wave in the Z direction is determined by the spatial increment $\sigma = -\operatorname{Im}\beta + \operatorname{Re}(\varepsilon h_\beta)$. The value of the transverse coordinate Z_{tr}, where the transition caused by the source of disturbances at a certain point Z_0 occurs, is evaluated by the e^N method in which the transition point is found from the equation

$$N = \int_{Z_0}^{Z_{\text{tr}}} \sigma \, dz = \sigma(Z_{\text{tr}} - Z_0).$$

Here the integral growth rate N is an empirical parameter, which takes the value $N = 10$ for small external perturbations. The distance to the transition point is estimated as $s = Z_{\text{tr}} - Z_0 = 10/\sigma$. For $Re < 520$, the flow on the leading edge is stable, i.e., $s = \infty$. With increasing Re, the increments increase and the distance s rapidly decreases. For instance, for $Re = 1000$ and a unit Reynolds number $Re_{\infty,1} = 23.4 \cdot 10^6$ m^{-1}, the amplification by a factor of e^{10} occurs at a distance of about 220 mm for the cylinders used in the experiment.

Measurement of the Shear Layer Thickness. In studying the evolution of natural disturbances and measuring the mean characteristics of the boundary layer on the attachment line of the circular cylinder, we used the following free-stream parameters: Mach number $M = 2$, unit Reynolds number $Re_1 = 6.8 \cdot 10^6$ m^{-1}, stagnation temperature $T = 280$ K, and free-stream velocity $U_\infty = 508$ m/sec.

The boundary-layer thickness was measured by a hot-wire anemometer with probe distances from the leading edge (apex) of the model $Z = 36$, 47, 58, and 85 mm. Based on the measurement results, we obtained profiles of the mean voltage $E(Y)/E_\infty$ and frequency-integral root-mean-square fluctuations of the mass flow rate $\langle \rho u \rangle$ as functions of the Y coordinate. The boundary-layer thickness δ was determined from the mean-voltage profile. The moment of drastic decrease in voltage corresponds to the upper boundary of the shear layer. For different values of Z, the boundary-layer thickness was constant: $\delta = (0.25 \pm 0.02)$ mm. The constancy of the boundary-layer thickness along the attachment line is in good agreement with the theory of [24]. The profiles of W and T (see Fig. 2) were obtained by data processing with the use of calibration dependences for the probe and known relations for flow parameters in a supersonic boundary layer [24]. Note, the profiles were measured beginning from the coordinate $Y = 0.05$ mm; nevertheless, for $Y < 0.15$ mm, the Reynolds number based on the wire diameter was $Re_d < 20$. According to [21], for instance, the calculation of the mean flow parameters on the basis of experimental points becomes incorrect for $Re_d < 20$ or $M < 1.3$ (these values are typical for hot-wire measurements in a supersonic flow). The first constriction can be weakened by increasing the unit Reynolds number, but the boundary-layer thickness decreases thereby; for $Y < 0.1$ mm, the hot-wire readings are affected by the wall, which leads to deviation of the profiles from the theoretical ones.

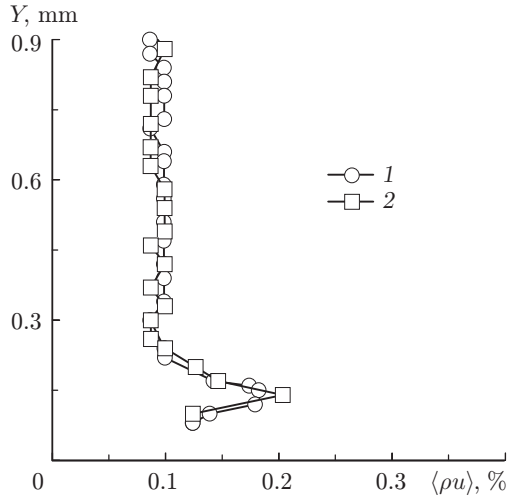

Fig. 5. Root-mean-square fluctuations of the mass flow rate in the shear layer for $Z = 85$ mm and $\mathrm{Re}_1 = 6.8 \cdot 10^6$ m^{-1}: points 1 and 2 show the experimental results obtained under identical conditions at different times.

Evolution of Disturbances in the Boundary Layer on the Attachment Line. According to flow-stability calculations, the Reynolds number obtained $\mathrm{Re} = 537$ is only slightly higher than the critical value $\mathrm{Re} \approx 520$, i.e., an insignificant increase in disturbances within the frequency range of 75–80 kHz can be observed in such experiments.

For $Y \approx 0.15$ mm, the distribution of root-mean-square fluctuations has a maximum (Fig. 5), which is typical of natural disturbances in the boundary layer. The amplitude of natural disturbances in the maximum of fluctuations increases with increasing coordinate Z. Based on the measured oscillograms, we obtained fluctuation spectra, which showed that disturbances in the frequency range from 1 to 30 kHz increase most intensely (almost fivefold). This fact can be explained by amplification of acoustic oscillations of the incoming flow by the supersonic boundary layer [25], though such calculations have not been performed yet.

To determine the flow character on the attachment line, the hot-wire probe was located at a distance $Z = 133$ mm. The unit Reynolds number was varied from $5 \cdot 10^6$ to $32 \cdot 10^6$ m^{-1}, which corresponded to the boundary-layer thickness of 0.26–0.10 mm. Since the measurement inside the boundary layer of small thickness are problematic, the flow character was determined by oscillograms of disturbances on the boundary-layer edge. It was assumed that the transition is accompanied by appearance of spikes on oscillograms, which is typical of the nonlinear stage of disturbance evolution. Since such a reconstruction of fluctuations was not observed, the boundary-layer flow, apparently, was laminar within the mentioned range of unit Reynolds numbers. The estimates of the transition position obtained by the e^N method also allow us to conclude that the flow character was laminar under given test conditions. The same measurements were performed on the long cylinder, using a Pitot probe mounted on the attachment line at a distance of 350 mm from the apex. The outer and inner sizes of the steel probe were 0.22×1.25 and 0.1×1.0 mm, respectively. It was found that the transition occurred at a unit Reynolds number $\mathrm{Re}_1 = 27 \cdot 10^6$ m^{-1} (or $\mathrm{Re} = 1070$). This value is rather close to the theoretical estimate given above.

Origin of a Turbulent Flow behind a Roughness Element. An earlier transition on the models usually occurs due to the presence of roughness elements (boundary-layer trips). According to [6–8], the dependence of the transition Reynolds number of the boundary layer on the attachment line on the roughness height k contains three typical regions. For smooth surfaces, where $k \ll \delta$, the transition is caused by development of unstable oscillations. For $k \approx \delta$, the transition Reynolds number depends significantly on the roughness height. For $k \gg \delta$, such a dependence is practically inexistent. For example, for subsonic flows with high roughness elements, the transition Reynolds number is $\mathrm{Re} = 240 \pm 20$.

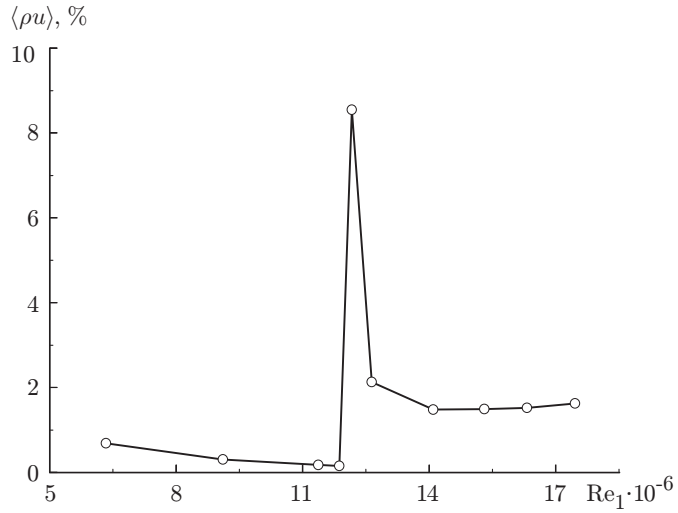

Fig. 6. Root-mean-square fluctuations of mass flow rate versus the unit Reynolds number for $Y = 0.15$ mm.

TABLE 1

k, mm	$\mathrm{Re}_1^* \cdot 10^{-6}$, m^{-1}	$(k/\eta)^*$	Re^*	X_1, mm	X_2, mm
0	27.0	0	1070	0	350
0.075	12.5	1.4	730	45	133
0.115	10.0	2.0	700	45	133
0.2	9.5	3.3	637	220	320
0.3	8.0	4.5	585	220	320
0.44	6.0	5.6	500	220	320
0.54	4.5	6.1	440	220	320
0.83	3.5	8.1	380	220	320
1.12	4.0	12	410	220	320

Note. Transition parameters are marked by the asterisk; X_1 and X_2 are the coordinates of the boundary-layer trip and hot-wire probe, respectively.

In our experiments, the height of the boundary-layer trips was chosen on the basis of Poll's diagram [8] constructed from experimental data for subsonic flow velocities. The experiments were performed for $\mathrm{Re}_1 = 5 \cdot 10^6$–$32 \cdot 10^6$ m^{-1}. As an example, we consider the measurement results for a boundary-layer trip of height $k = 0.075$ mm. In this case, the boundary-layer flow along the attachment line remained laminar up to $\mathrm{Re}_1 = 10^7$ m^{-1}. For $\mathrm{Re}_1 = 12.5 \cdot 10^6$ m^{-1}, a hybrid (nonlinear) regime was observed, typical of the transitional region in the boundary layer [26]. With further increase in Re_1, the boundary-layer flow became turbulent. For this roughness height, the transition curve obtained from root-mean-square fluctuations is plotted in Fig. 6. This curve has a clear peak corresponding to the nonlinear transition region behind which the flow becomes turbulent. The same conclusion can be drawn by analyzing disturbance spectra and oscillograms. Since these measurements were performed with a fixed probe position relative to the model surface ($Y = 0.1$ mm), we performed additional measurements, which showed that the result depends weakly on Y. Thus, the transition with a boundary-layer trip of height $k = 0.075$ mm occurs at $\mathrm{Re}_1 = 12.5 \cdot 10^6$ m^{-1}.

Similar data were obtained for other wire diameters. The origin of a turbulent flow was accompanied by a substantial increase in boundary-layer thickness. Thus, for $k = 0.115$ mm, the critical regime corresponded to a unit Reynolds number $\mathrm{Re}_1 = 9.5 \cdot 10^6$ m^{-1}. For $\mathrm{Re}_1 = 9.3 \cdot 10^6$ m^{-1} and $Z = 115$ mm, the mean and fluctuating profiles of the boundary layer were measured. A significant (up to $\delta \approx 1$ mm) increase in boundary-layer thickness was obtained.

The data for transition on the attachment line behind roughness elements, which were measured in the present work, are listed in Table 1 and compared with the data of [6, 27] in Fig. 7. In contrast to [27], we managed to obtain transition curves in the present experiments, which was achieved by continuous variation of the unit Reynolds number [for a given height of the boundary-layer trip, the dependence $\mathrm{Re}(k/\eta)$ is linear].

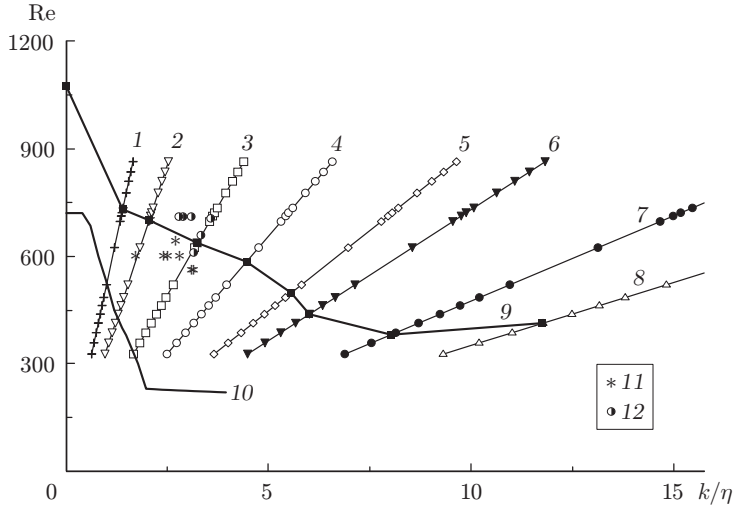

Fig. 7. Transition diagram on a swept cylinder for $k = 0.075$ (1), 0.115 (2), 0.2 (3), 0.3 (4), 0.44 (5), 0.54 (6), 0.83 (7), and 1.12 mm (8); curve 9 refers to data of the present work for M = 2 and curve 10 refers to data of [6], and points 11 and 12 refer to data of [27] for a laminar and turbulent flows, respectively.

Conclusions. Stability of the boundary layer on the attachment line is theoretically analyzed within the framework of the asymptotic method of multiple scales. The asymptotic solution is shown to be in good agreement with the exact solution for two-dimensional disturbances corresponding to the HMP mode with allowance for flow compressibility. It is found that oblique waves are most unstable in a supersonic flow.

The laminar–turbulent transition in the boundary layer on the attachment line on a swept cylinder mounted at an angle of 68° behind two-dimensional roughness elements in the form of wires 0.075–1.120 mm in diameter and without them for M = 2 is experimentally studied. The critical Reynolds numbers of boundary-layer transition are determined. The results of the present work are in agreement with the data obtained in NASA (Ames) for M = 1.6 and a sweep angle of 76° and supplement the latter.

It is shown that the transition Reynolds numbers on the attachment line of the swept cylinder in the supersonic flow are higher than those in the subsonic flow, in all flow regimes. The difference observed seems to be related to the high level of turbulence in Poll's experiments and the low noise of the supersonic flow in [27] and in the present work.

This work was supported by the International Science and Technology Center (Grant No. 128-96).

REFERENCES

1. W. Pfenninger, "Flow phenomena at the leading edge of swept wings," in: *Recent Developments in Boundary Layer Research*: AGARDograph 97, Part 4 (1965).
2. M. Gaster, "On the flow along swept leading edges," *Aeronaut. Quart.*, **18**, Part 2, 165–184 (1967).
3. W. Pfenninger, "Laminar flow control — laminarization," in: *Special Course on Concepts for Drag Reduction*: AGARD-R-654, 3-1–3-75 (1977).
4. C.-J. Woan and P. B. Gingrich, "CFD validation of a supersonic laminar flow control concept," AIAA Paper No. 91-0188 (1991).
5. M. Gaster, "A simple device for preventing turbulent contamination on swept leading edges," *J. Roy. Aeronaut. Soc.*, **69**, 788 (1965).
6. D. I. A. Poll, "Transition in the infinite swept attachment line boundary layer," *Aeronaut. Quart.*, **30**, 607 (1979).
7. D. I. A. Poll, "The development of intermittent turbulence on the swept attachment line including the effects of compressibility," *Aeronaut. Quart*, **34**, 1–23 (1983).
8. D. I. A. Poll, "Transition description and prediction in three-dimensional flows," in: *Special Course on Stability and Transition of Laminar Flow*: AGARD-R-709, 5-1–5-23 (1984).

9. P. Hall, M. R. Malik, and D. I. A. Poll, "On the stability of an infinite swept attachment line boundary layer," *Proc. Roy. Soc. London, Ser. A*, **395**, 229–245 (1984).
10. W. Pfenninger and J. W. Bacon, "Amplified laminar boundary layer oscillations and transition at the front attachment line of a 45 flat-nosed wing with and without boundary layer suction," in: *Viscous Drag Reduction*, Plenum Press, New York (1969).
11. R.-S. Lin and M. R. Malik, "The stability of incompressible attachment line boundary layers: A 2D eigenvalue approach," AIAA Paper No. 94-2372 (1994).
12. A. V. Kazakov, "Effect of surface temperature on stability of the boundary layer on the attachment line on a swept wing," *Izv. Akad. Nauk SSSR, Mekh. Zhidk. Gaza*, No. 6, 78–82 (1990).
13. A. V. Kazakov, "Effect of surface temperature on stability of a supersonic boundary layer on the attachment line on a swept wing," *Izv. Ross. Akad. Nauk, Mekh. Zhidk. Gaza*, No. 5, 43–49 (1997).
14. A. V. Kazakov, "Effect of energy addition on boundary-layer stability on the attachment line on a swept wing at supersonic velocities," *Izv. Ross. Akad. Nauk, Mekh. Zhidk. Gaza*, No. 5, 90–97 (1998).
15. P. Hall and M. R. Malik, "On the stability of a three dimensional attachment-line boundary layer: Weakly nonlinear theory and numerical approach," *J. Fluid Mech.*, **163**, 257–282 (1986).
16. P. R. Spalart, "Direct numerical study of leading edge contamination," AGARD CP, No. 438 (1988).
17. R. D. Joslin, "Direct simulation of evolution and control of nonlinear instabilities in attachment-line boundary layers," AIAA Paper No. 94-0826 (1994).
18. G. I. Bagaev, V. A. Lebiga, V. G. Pridanov, and V. V. Chernykh, "T-325 low-turbulent supersonic wind tunnel," in: *Aerophysical Research* (collected scientific papers) [in Russian], Novosibirsk (1972), pp. 11–13.
19. V. A. Lebiga, "Measurement of turbulence characteristics in compressible flows," in: *Methods and Techniques of Aerophysical Research* (collected scientific papers) [in Russian], Novosibirsk (1978), pp. 44–56.
20. A. D. Kosinov, N. V. Semionov, and Yu. G. Yermolaev, "Disturbances in test section of T-325 supersonic wind tunnel ITAM SB RAS," Preprint No. 6-99, Inst. Theor. Appl. Mech., Sib. Div., Russian Acad. of Sci., Novosibirsk (1999).
21. A. J. Smits, K. Hayakawa, and K. C. Muck, "Constant-temperature hot wire anemometer practice in supersonic flows. Part 1. The normal wire," *J. Exp. Fluids*, **1**, 83–92 (1983).
22. V. N. Zhigulev and A. M. Tumin, *Initiation of Turbulence* [in Russian], Nauka, Novosibirsk (1987).
23. A. H. Nayfeh, "Stability of three-dimensional boundary layers," *AIAA J.*, **18**, No. 4, 406–416 (1980).
24. G. Schlichting, *Boundary Layer Theory*, McGraw-Hill, New York (1968).
25. S. A. Gaponov, "Interaction of a supersonic boundary layer with acoustic disturbances," *Izv. Akad. Nauk SSSR, Mekh. Zhidk. Gaza*, No. 6, 51–56 (1977).
26. A. I. Semisynov, V. E. Novikov, N. V. Semionov, et al., "Experimental study of transition conditions on a swept cylinder in a supersonic flow," Preprint No. 4-2000, Inst. Theor. Appl. Mech., Sib. Div., Russian Acad. of Sci., Novosibirsk (2000).
27. C. P. Coleman, D. I. A. Poll, J. A. Laub, and S. W. D. Wolf, "Leading edge transition on a 76 degree swept cylinder at Mach 1.6," AIAA Paper No. 96-2082 (1996).